Torque and dynamics of linking number relaxation in stretched supercoiled DNA

John F. Marko
Department of Physics and Astronomy and Department of Biochemistry, Molecular Biology and Cell Biology, Northwestern University, Evanston, Illinois 60208, USA

(Received 24 April 2007; revised manuscript received 27 June 2007; published 29 August 2007)

In micromechanical studies of DNA, plectonemically supercoiled domains are often used as sources of constant torque. These torques are not easily measured and are instead usually estimated. Here, coexisting extended and supercoiled DNA domains are analyzed, and closed-form expressions for the dependence of extension and torque on force and linking number are presented. When there are coexisting domains of plectonemic and extended DNA, the torque depends only on force, with no dependence on linking number. However, torque depends on force in a manner more complex than a simple power law, involving the free energy of the extended and plectonemic DNA. A simple strategy is described for measurement of the free energies of both extended and plectonemic DNA without reference to specific microscopic polymer models. Applications of the theory to analysis of relaxation of supercoiling by enzymes which permit friction-controlled rotational relaxation of linking number is also presented. Such enzymes must display a breaking of symmetry between relaxations driven by equal magnitude but opposite direction torques.

DOI: 10.1103/PhysRevE.76.021926 PACS number(s): 87.14.Gg, 82.35.Pq, 87.15.Aa, 87.15.La

I. INTRODUCTION

Single-molecule DNA stretching is useful for studying not only DNA itself, but also for the study of proteins that interact with the double helix. Many such experiments have followed from the seminal work of Smith *et al.* [1]. The semiflexible polymer model provides a quantitative starting point for theories describing these types of experiments [2–5]. This model, which describes DNA bending fluctuations in terms of a single "persistence length," describes a wide range of experiments thanks to the separation of the double-helix persistence length (50 nm) from both the base-pair (bp) scale (0.34 nm) and the total molecular length scale (>1000 nm for >3 kilobase molecules). The availability of a simple but quantitative theoretical framework for DNA elasticity has greatly facilitated analysis of a wide variety of single-molecule-DNA-based experiments.

DNA's double-helix structure gives it a twist modulus. Both the twisting elasticity and the topology of wrapping of the DNA strands in the double helix are of paramount biological importance, with a wide range of enzymes known to play roles in control of the DNA linking number *in vivo*. Elegant experimental techniques have been developed to control the linking numbers of individual DNA molecules, and quantitative studies have been made of the elasticity of twisted DNA molecules [6–9]. Precise measurements of elasticity of twisted DNA molecules have been used as the basis of studies of enzymes whose interactions with DNA depend on that twisting, most notably topoisomerases, which mediate quantized changes in DNA linking number [10–15]. Such enzymes are affected by torques in DNA on the order of a few k_BT or pN nm (1 pN=1 piconewton=10^{-12} newton; $1k_BT=4.1$ pN nm at $T=300$ K).

A dominant feature of the elastic behavior of twisted DNA is that, at fixed force, introduction of sufficient linking number to a DNA molecule causes it to start to wrap around itself or *supercoil* in the manner of a twisted wire. This buckling is driven by the reduction of twist elastic energy occurring when linking number is transferred to chiral bending, or "writhe." Further introduction of linking number causes folding up of the molecule into a plectonemic supercoiled DNA, and a gradual reduction in molecule extension. This folding can be discussed in terms of coexisting domains of extended and supercoiled DNA [16–24]. An important feature of this phase-coexistence-like behavior is that, while the linking number is converting DNA between plectonemic and extended forms at constant force, the torque in the molecule is constant [8,9].

Almost all DNA-twisting experiments have used either a magnetic particle that can be rotated by rotating a magnetic field [6], or a mechanically rotating cantilever [25], to control DNA linking number. Such experiments work in an ensemble of fixed linking number, forcing experimenters to estimate torques indirectly [8,9]. Recently, a few experiments have used either rotational drag [26] or rotated-polarization laser trapping [27] to more directly monitor torques in DNA, and over the next few years comprehensive studies of the torque dependence of DNA structure and elasticity and also of how torques affect protein-DNA interactions are likely to be carried out. Given this, it will be useful to have a simple and quantitative theory of the elasticity of twisted DNA, with a focus on the DNA torque associated with a given applied force and linking number.

Here, an analytical theory of the elasticity of twisted DNA molecules is constructed, incorporating a number of different theoretical elements. A main objective is to provide a simple but quantitative closed-form analytical description of the coexistence of extended and plectonemically supercoiled domains of DNA (Sec. II). This problem has been studied using a variety of analytical and semianalytical methods [16–23]. However, previous works have not provided closed-form expressions for DNA extension and torque at constant force, across the range of DNA linking number that is accessible in magnetic tweezer experiments, including twist-stiffness-screening effects of chiral fluctuations in the extended DNA [31,32], and considering effects of DNA denaturation [17].

In this paper, a simple free energy model of the plectonemic supercoil known to describe both real and simulated DNA rather accurately [28–30] is combined with the free energy of extended twisted DNA [31,32], to obtain a closed-form theory for the coexistence of extended and supercoiled DNA. An important result is a closed-form computation of torque as a function of force and linking number. However, this model also suggests a general framework for analysis of experiments on twisted DNA.

Calculations of Sec. II use a mean-field approximation for the phase coexistence. In Sec. III this is tested by comparing the analytical results to those from a Monte Carlo computer simulation using an established method [24].

If DNA is sufficiently under- or overtwisted, the two strands will separate from one another, or "melt." In Sec. IV this effect is included using a simple approach. A low-force force-torque "phase diagram" is obtained, which provides a unified description of the highly asymmetric denatured DNA states found for under- and overtwisting [25,33,34].

Finally, in Sec. V the related problem of analysis of how linking number and torque in DNA are relaxed by type-I topoisomerase enzymes is discussed. Recent experiments [14] have revealed that the rotary relaxation that occurs is dominated by molecular friction. The relation between angular velocity and torque for a model of an enzyme which catalyzes release of internal linking number by a frictionally controlled rotation mechanism is discussed. The model of Sec. V is similar to that of Koster *et al.* [14], but includes some features necessary to make it thermodynamically consistent. An important general result is that, while the linear rotary friction must be independent of the rotation direction, the nonlinear friction must differ for the two directions of rotation.

II. COEXISTENCE OF DNA STATES

Consider a DNA molecule stretched by force f, and how its free energy and structure change as its linking number is changed by an amount $\Delta\mathrm{Lk}$ away from its relaxed linking number Lk_0. The free energy will be described intensively on a per length basis. The linking number will also be described intensively using the conventional linking number density $\sigma \equiv \Delta\mathrm{Lk}/\mathrm{Lk}_0$. Here Lk_0 is the linking number of the relaxed double helix, which turns through one helix repeat every relaxed molecule contour length of 3.6 nm (10.5 bp). The contour-length rate of rotation of the relaxed double helix, $\omega_0 \equiv 2\pi/(3.6\ \mathrm{nm}) = 1.85\ \mathrm{nm}^{-1}$, will be used to convert σ to an angle of rotation per contour length.

The DNA molecule is considered to be formed into domains of two "pure" states, each of which is described by a free energy per molecular length, dependent on the applied force f and the linking number density σ. As the forces on the two domains are equal, the focus will be on the σ dependences of the two states, which in most of this paper will describe "stretched" and "plectonemic" DNA [16–23].

The free energies per length of the two pure states are therefore $\mathcal{S}(\sigma)$ (for stretched DNA) and $\mathcal{P}(\sigma)$ (plectonemic DNA). These free energies are $-k_BT$ times the logarithm of the partition function for the molecule at fixed force and linking number, divided by the relaxed double-helix contour length (note that all the free energies per length of this paper can be converted to free energies per base pair by multiplying by 0.34 nm/bp). For the pure states, the rate at which work is done injecting linking number is proportional to the torque:

$$\tau = \frac{1}{\omega_0}\frac{\partial \mathcal{S}(\sigma)}{\partial \sigma}. \tag{1}$$

The prefactor converts the σ derivative to one with respect to rotation angle; a similar equation holds for the $\mathcal{P}$ state.

Along a molecule which is a fraction x_s of state $\mathcal{S}$ and a fraction $x_\mathrm{p} = 1 - x_\mathrm{s}$ of state $\mathcal{P}$, the free energy per base pair of the mixed phase is

$$\mathcal{F}(\sigma) = x_\mathrm{s}\mathcal{S}(\sigma_\mathrm{s}) + x_\mathrm{p}\mathcal{P}(\sigma_\mathrm{p}). \tag{2}$$

The equilibrium length fraction x_s and the free energy are determined by minimization of this free energy subject to the constraint $\sigma = x_\mathrm{s}\sigma_\mathrm{s} + x_\mathrm{p}\sigma_\mathrm{p}$.

If the two pure state free energy densities plotted as a function of linking number density never cross, then one pure state or the other will be the equilibrium state, i.e., one of the two extreme cases $x_\mathrm{s} = 0$ or $x_\mathrm{s} = 1$ will always minimize Eq. (2). However, if the two free energy densities cross, then there will be a range of σ over which there will be coexisting domains of the two states. Figure 1 shows this situation, sketched to correspond to the case of main interest here, where at low values of σ the stretched state is stable (lower in free energy) relative to the plectoneme state, but where at large σ the stability reverses due to "screening" of the twist energy by the plectonemic state's writhe [16–18,20].

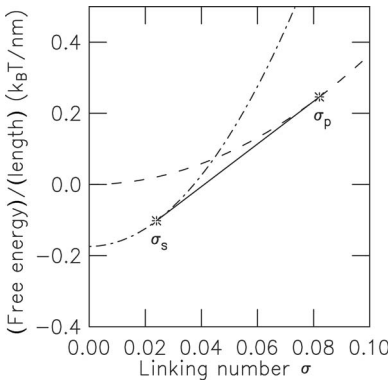

FIG. 1. Free energies of extended [dot-dashed curve, $\mathcal{S}(\sigma)$] and plectonemic supercoil [dashed curve, $\mathcal{P}(\sigma)$] DNA states as a function of linking number σ. For $\sigma < \sigma_\mathrm{s}$, the $\mathcal{S}$ state is lower in free energy than either $\mathcal{P}$ or any mixture of the two. Similarly, for $\sigma > \sigma_\mathrm{p}$, pure $\mathcal{P}$ is the lowest free energy configuration. However, for σ between σ_s and σ_p the tangent construction shown (solid line segment between tangent points indicated by stars), representing coexisting domains of $\mathcal{S}(\sigma_\mathrm{s})$ and $\mathcal{P}(\sigma_\mathrm{p})$, is the lowest free energy state. Note that the gap between the two states at $\sigma = 0$ is the free energy difference between random coil DNA [$\mathcal{P}(0)$] and stretched unsupercoiled DNA [$\mathcal{S}(0)$]; this difference grows with applied force.

Minimization of Eq. (2) is accomplished by a double-tangent construction familiar from other examples of phase coexistence (e.g., liquid-gas); in this case the conserved density is that of linking number (Fig. 1). The two coexisting states of linking number densities σ_s and σ_p satisfy $\partial\mathcal{S}(\sigma_s)/\partial\sigma_s=\partial\mathcal{P}(\sigma_p)/\partial\sigma_p$, i.e., they have equal torques. They mix in proportions x_s and x_p, so the free energy in the coexistence region is

$$\mathcal{F}(\sigma)=\mathcal{S}(\sigma_s)+\frac{\partial\mathcal{S}(\sigma_s)}{\partial\sigma_s}(\sigma-\sigma_s)=\mathcal{P}(\sigma_p)+\frac{\partial\mathcal{P}(\sigma_p)}{\partial\sigma_p}(\sigma-\sigma_p). \tag{3}$$

In the coexistence region, the fractions of the two states in the mixed state depend linearly on σ, as

$$x_s=\frac{\sigma_p-\sigma}{\sigma_p-\sigma_s},\quad x_p=\frac{\sigma-\sigma_s}{\sigma_p-\sigma_s}. \tag{4}$$

The coexistence construction guarantees that the free energy is a convex function of linking number, and therefore that the torque is a monotonic function of linking number, as required for mechanical stability. In the coexistence region (σ between the limits σ_s and σ_p) the torques in the two types of domains are equal and σ independent; i.e., the σ derivative of Eq. (3) is constant.

In the coexistence region Eq. (4) indicates that the rate of change of the length fractions with σ is constant: $\partial x_s/\partial\sigma=-1/(\sigma_p-\sigma_s)$. This generates the linear dependence of the molecule extension on linking number observed experimentally once the threshold for generating plectonemic DNA is reached, as can be seen by computing the molecule extension (as a fraction of relaxed double-helix contour length L):

$$\frac{z}{L}=-\frac{\partial\mathcal{F}}{\partial f}=-x_s\frac{\partial\mathcal{S}(\sigma_s)}{\partial f}-x_p\frac{\partial\mathcal{P}(\sigma_p)}{\partial f}. \tag{5}$$

In the coexistence region, the only σ dependence is the linear variation of x_s and x_p, making the dependence of extension on σ entirely linear.

In the main case of interest here where $\mathcal{P}$ is the plectonemic supercoil state, its zero length eliminates its contribution to Eq. (5) (i.e., $\partial\mathcal{P}/\partial f=0$), yielding

$$\frac{z}{L}=-x_s\frac{\partial\mathcal{S}(\sigma_s)}{\partial f}=\frac{\sigma_p-\sigma}{\sigma_p-\sigma_s}\frac{z(\sigma_s)}{L}, \tag{6}$$

where the final extension per length factor is the extension per length of the extended DNA state.

Experimentally, σ_s and σ_p can be measured from the beginning and the end of the linear coexistence regime of extension as a function of σ. Likewise, $z(\sigma_s)/L$ is the extension per length of the molecule at the onset of the linear regime. Thus Eq. (6) can be used to determine the coexisting state linking number values, the extension of the stretched DNA state as a function of force and linking number, and via integration the free energy of the stretched state. Then through use of the tangent construction (Fig. 1), the free energy of the plectonemic state can be measured. Note that when the molecule is entirely converted to plectoneme ($x_s=0$, $x_p=1$) the extension reaches zero. The point $\sigma=\sigma_p$ where this occurs can be estimated experimentally from extrapolation of the extension data to zero.

A. Plectonemically supercoiled DNA

When DNA is under zero tension and sufficient torsional stress (sufficient change in linking number away from the relaxed state), an interwound plectonemic supercoil is formed. Thermal fluctuations oppose formation of this interwound structure so that there is effectively a threshold of $|\sigma|\approx 0.01$ required to form it [16,17,21]; this threshold corresponds to the point where roughly one unit of ΔLk has been injected per twist persistence length C, i.e., the point at which the torsional stress in the molecule overcomes random fluctuations of torsional stress.

Without any chiral bending all of the linking number change must be in twist and the free energy will correspond to the twist energy for a total twist angle of $2\pi\Delta$Lk. Beginning with a harmonic twist energy as encountered in the theory of twisted elastic rods [35], which has been shown to apply to DNA for small linking number changes in direct micromechanical measurements, the twist energy per length is

$$\mathcal{E}_{\text{twist}}(\sigma)=\frac{k_BTC}{2}\left(\frac{2\pi\Delta\text{Lk}}{L}\right)^2=\frac{k_BTC\omega_0^2}{2}\sigma^2=\frac{c}{2}\sigma^2 \tag{7}$$

where C is the twist persistence length of DNA (so that k_BTC is the twist rigidity elastic constant [35]). It will simplify calculations to define $c\equiv k_BTC\omega_0^2$.

Although there remains some disagreement between different analyses of experimental data [36], most researchers now agree that $C=95\pm10$ nm [23,26,31,32,36] for DNA in physiological buffers with univalent salts in the 10–200 mM range. This value is somewhat higher than older estimates in the $C=75$ nm range [29], possibly because of the renormalization of twist rigidity by bending fluctuations [31,32]. It should be noted that there is some evidence for there being an appreciable suppression of the twist rigidity to $\approx$85 nm by 5 mM Mg^{2+} ions [23], and that in general one can expect some variation of DNA mechanical properties with solution conditions, and applied forces.

However, since linking number becomes largely absorbed into writhe, the free energy drops well below the pure twist energy [16,17]. Accounting for effects of chiral fluctuations, bending at plectoneme tips, thermal fluctuations of branching of the superhelix, and effects of self-avoidance starting from microscopic polymer or elastic models is possible but already quite complex (e.g., Refs. [16,17,21–23]). Here this issue is simplified by employing results of Klenin, Rybenkov, and Vologodskii [28–30] which have empirically established the free energy of supercoiled DNA to be well described by a quadratic model similar in form to Eq. (7):

$$\mathcal{P}(\sigma)=\frac{k_BTP}{2}\left(\frac{2\pi\Delta\text{Lk}}{L}\right)^2=\frac{k_BTP\omega_0^2}{2}\sigma^2=\frac{p}{2}\sigma^2, \tag{8}$$

where P (alternately $p\equiv k_BTP\omega_0^2$) describes the twist stiffness of the plectonemic state. Generation of writhe reduces the free energy so $P<C$. The torque of the $\mathcal{P}$ state is, by Eq.

(1), $\tau=(p/\omega_0)\sigma=k_BTP\omega_0\sigma$. Finally, the $\mathcal{P}$ state, since it is contracted so that its ends are coincident, does not have any force dependence; its length is zero.

Available data indicate that P in the range 21–27 nm [28–30] describes the free energy of supercoiled DNA, for salt concentrations in the range relevant to most biochemistry experiments. The stiffness P varies with salt concentration, since that in turn adjusts the effective diameter of the double helix; for higher salt, P is reduced, while for lower salt P increases. This effect, analyzed in detail by Klenin, Rybenkov, and Vologodskii [28–30], arises because bending energy in a plectonemic superhelix is reduced when the DNA effective diameter is reduced.

For high and low salt concentrations, the plectoneme free energy ceases to behave quadratically for $|\sigma|>0.04$. For high salt concentrations (>200 mM univalent salt, or a few-millimolar concentrations of divalent cations), the tight superhelices that form cause the free energy to grow substantially more slowly than quadratically in $|\sigma|$. For low salt concentrations (<5 mM univalent salt) the relatively strong electrostatic repulsion between double-helix segments forces more linking number into twist as $|\sigma|$ is increased, causing the free energy to grow slightly faster than quadratically with $|\sigma|$. Addition of higher-order σ^3 and σ^4 terms into Eq. (8) can allow these effects to be quantitatively included.

For univalent salts in the 10–100 mM range ("physiological" conditions are thought to be ≈100–200 mM), the effective DNA diameter is ≈5–15 nm [30], and these different effects conspire to produce a nearly quadratic dependence of plectonemic free energy on $|\sigma|$ [28,29], over a rather wide range of σ (–0.04 to +0.1). In part, this range is wide because the twist is strongly reduced by writhe for the plectonemic supercoil.

In this paper $P=24$ nm will be used, which provides a good description of plectonemic free energy over a wide range of σ for 200 mM univalent salt conditions, except for a comparison with 10 mM Na^+ experimental data, where the value $P=28$ nm [30] will be used. Results of Rybenkov *et al.* [30] and Klenin *et al.* [28,29] can be used to choose P for most biologically relevant combinations of univalent and divalent cations.

B. Extended DNA under torsional stress

When sufficient force is applied to DNA under torsional stress it will become extended, but will be subject to chiral fluctuations [16,17,31,32]. The free energy of the extended DNA at a fixed force f can be written as an expansion in σ [20,31,32]:

$$\mathcal{S}(\sigma) = -g + \frac{c_s}{2}\sigma^2. \tag{9}$$

The free energies g and c_s are measurable functions of force. The leading constant $-g$ is the free energy of stretched, nicked (freely swiveling) DNA. From an experimental point of view, g can be determined by integration of extension vs force, using $z/L=\partial g/\partial f$ [5]. The twist stiffness of the extended DNA state is described by c_s, which can be measured from the curvature of the extension as a function of σ near its maximum.

The first two terms of the expansion of Eq. (9) are sufficient to illustrate the basic properties of state coexistence in a quantitative way. As for the plectonemic state, higher-order terms can be added (e.g., σ^3 to generate positive-negative twisting asymmetry).

A more general expansion would replace σ with $\sigma-\sigma_0$ in Eq. (9), where this additional force-dependent σ_0 parameter sets the linking number at which the double helix is relaxed. Variation of σ_0 with force takes into account the stretch-twist coupling. However, for the relatively low forces of interest here (a few piconewtons), this coupling has only weak effects and may be neglected (i.e., $\sigma_0\approx 0$). For a given force, σ_0 is easily determined by finding the σ value at which a local maximum of extension is obtained. Here, $\sigma_0=0$ is assumed for the $\mathcal{S}$ state.

In this paper, established polymer-statistical-mechanical results for g and c_s will be used, which have been shown to describe experiments quantitatively [5,31,32]:

$$g = f - \left(\frac{k_BTf}{A}\right)^{1/2},$$

$$c_s = c\left[1 - \frac{C}{4A}\left(\frac{k_BT}{Af}\right)^{1/2}\right]\sigma^2. \tag{10}$$

The expression for g is the first two terms of the high-force expansion of the free energy of the semiflexible polymer including stretching elasticity [5]. While an exact expression can be numerically calculated [5] this large-force expansion is sufficient for this paper, as it provides a good description of DNA stretching free energy for forces sufficient to substantially stretch the molecule (>0.2 pN) but insufficient to disrupt its secondary structure (<10 pN).

The form of c_s follows from that calculated perturbatively for large forces and small torques for the semiflexible polymer with harmonic twist rigidity by Moroz and Nelson [31,32] (the precise form of c_s used here is discussed in Refs. [20,37]). The main effect introduced by c_s is a force dependence of the twisting rigidity. Reducing force reduces c_s since more linking number can be absorbed into writhe fluctuations at lower forces [31,32]. Both g and c_s have units of energy per length (as do c and p).

If one wants to include the effect of double-helix stretching, this may be done by including a term $f^2/(2f_0)$ in Eq. (10), with stretching elastic constant $f_0\approx 1200$ pN. However, for forces below 10 pN this term has negligible effects.

Although not pursued in this paper, the coefficients g and c_s (and a possible similar coefficient coupled linearly to σ) could be considered as quantities to be determined from experimental extension vs force data. The results could then be compared with specific models, e.g., the result of the inextensible semiflexible polymer with twist stiffness of Eq. (10).

C. Single-state and coexistence regions

With these simple expressions for plectonemic and extended DNA free energies, the state coexistence behavior can

be computed. The force f is considered to be constant, and the focus below will be mainly on the σ dependence. The mixed-state free energy is simply

$$\mathcal{F} = x_s\left(-g + \frac{c_s\sigma_s^2}{2}\right) + x_p\frac{p\sigma_p^2}{2} \tag{11}$$

where the state fractions satisfy $x_s+x_p=1$, and where the linking numbers satisfy $\sigma=x_s\sigma_s+x_p\sigma_p$. Eliminating x_p and σ_p, and then determining the value of σ_s by minimization ($\partial\mathcal{F}/\partial\sigma_s=0$) yields

$$\sigma_s = \frac{p}{x_s p + x_p c_s}\sigma. \tag{12}$$

Similarly, the equilibrium value of x_s is determined by solving $\partial\mathcal{F}/\partial x_s=0$; elimination of σ_s by Eq. (12) gives

$$x_s = \frac{1}{1-p/c_s} - \left(\frac{p}{2(1-p/c_s)g}\right)^{1/2}|\sigma|. \tag{13}$$

Note that $p<c_s$ is required to solve Eq. (13); $\mathcal{P}$ must become lower than $\mathcal{S}$ for some σ for coexistence to occur. If $c_s<p$, $\mathcal{S}$ will always be below $\mathcal{P}$, and the pure state $x_s=1$ will always be the equilibrium. The $|\sigma|$ in Eq. (13) arises from a physically appropriate choice of the branch of the square root. The linear dependence of the state fraction on linking number is obtained as anticipated in Eq. (4) for both signs of σ.

Coexisting-state linking number densities may be calculated from Eq. (4):

$$|\sigma_s| = \frac{1}{c_s}\left(\frac{2pg}{1-p/c_s}\right)^{1/2},$$

$$|\sigma_p| = \frac{1}{p}\left(\frac{2pg}{1-p/c_s}\right)^{1/2}. \tag{14}$$

Since σ_s can be determined from experimental data by determining where the linear (coexistence) regime begins, and since the slope $dx_s/d\sigma$ is similarly determined from experimental data, and finally, since g is independently well known, it is possible to determine the stiffnesses c_s and p. This would amount to a measurement of the free energy of extended and plectonemic DNA in a way relatively independent of details of specific microscopic theories.

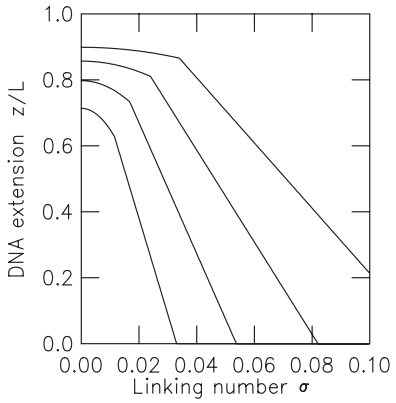

FIG. 2. Extension versus linking number, for forces 0.25 (lowest curve), 0.5, 1.0, and 2.0 pN (highest curve), for positive linking number change ($\sigma>0$). As the force is increased, the extension increases, and the effect of torsional stress (linking number) is reduced. Parameter values are $C=95$ nm, $A=50$ nm, $P=24$ nm. The parabolic peak of each extension curve occurs when the DNA is pure extended state; extended and plectonemic DNA are in coexistence on the linear part of each extension curve. The beginning of the linear segments indicates σ_s, and their σ intercepts indicate σ_p.

Equation (14) immediately gives the torque, via Eq. (1) and either of the pure-state free energies Eq. (8) or Eq. (9):

$$\tau = \begin{cases} (c_s/\omega_0)\sigma, & |\sigma| < |\sigma_s|, \\ [2pg/(1-p/c_s)]^{1/2}/\omega_0, & |\sigma_s| < |\sigma| < |\sigma_p|, \\ (p/\omega_0)\sigma, & |\sigma| > |\sigma_p|. \end{cases} \tag{15}$$

For constant force, as $|\sigma|$ is increased from zero, the equilibrium state is first pure extended DNA, with torque growing linearly with $|\sigma|$. Then at $\sigma=\sigma_s$, the coexistence point is reached, and until $\sigma=\sigma_p$ the torque is constant. Finally, for $|\sigma|>|\sigma_p|$, the entire DNA molecule is a plectonemic supercoil, and again the torque changes with $|\sigma|$ but at a reduced rate (recall $P<C_s$) due to the efficient removal of twist by the large plectonemic writhe.

The equilibrium free energy can also be computed as a function of force and linking number:

$$\mathcal{F} = \begin{cases} -g + \frac{1}{2}c_s\sigma^2, & |\sigma| < |\sigma_s|, \\ -g/(1-p/c_s) + [2pg/(1-p/c_s)]^{1/2}|\sigma|, & |\sigma_s| < |\sigma| < |\sigma_p|, \\ \frac{1}{2}p\sigma^2, & |\sigma| > |\sigma_p|. \end{cases} \tag{16}$$

In the coexistence region, the linear dependence of the free energy on σ generates the constant torque of Eq. (15).

Figure 2 shows extension versus linking number for this model via Eq. (5). The curves are computed for $f=0.25$ (lowest curve), 0.5, 1.0, and 2.0 pN (highest curve), for stiffnesses $A=50$ nm, $C=95$ nm, and $P=24$ nm. The parabolic

peak at the top of each curve shows the region of pure extended DNA. This joins to a linear coexistence segment which stretches between σ_s and σ_p, the latter being the point where extension reaches zero. The curves have the characteristic "hat" shape seen experimentally [9].

D. Torque dependence on force

A main result of this paper is the middle line of Eq. (15) which gives the dependence of the coexisting state torque on force:

$$\tau = \sqrt{\frac{2k_BTPg}{1 - P/C_s}}. \tag{17}$$

The torque is now given in terms of the twist stiffnesses of the plectoneme (P) and of the extended state $C_s = C[1-(C/2)(k_BT/4A^3f)^{1/2}]$ (note that $C_s/C = c_s/c$ and $P/C_s = p/c_s$). Since these stiffnesses are independently known [28,31,32], Eq. (17) amounts to a prediction for future experiments that will directly measure torques.

The force dependence of the torque enters mainly through the extended-state free energy $g = f - (k_BTf/A)^{1/2} \approx f$ in the numerator. However, note that the twist persistence length of the extended state C_s increases with increasing force.

The simplest application of Eq. (17) is in estimating torques in situations where one is in the coexistence range of σ and where one knows the force. This is commonly the case in magnetic tweezer experiments, where force and linking number are both fixed by the fixed position of a macroscopic magnet [9]. An elegant example of use of this is the constant-torque driving of rotational relaxation of DNA [14]. One must be in the coexistence range of σ in order to have this constant torque; below σ_s, the torque will drop below the coexistence value, and above σ_p the torque will increase with $|\sigma|$.

It is instructive to consider the situation of fixed σ and varied force. This is experimentally accessible using various micromanipulation schemes, including magnetic tweezers as long as the force is not reduced to so low a value that linking number can leak away by having the DNA hop over the bead. Imagine holding σ fixed at a value sufficient to form plectonemic supercoils at a low force, and then slowly increase f.

At low forces, the entire molecule will remain supercoiled (with torque equal to $\tau = \tau_p = k_BTP\omega_0\sigma$) until the force reaches a threshold value f_p, i.e., until the work done by the external force can overcome the plectoneme's "length binding energy"[16,17]. This effect can be analyzed using Eq. (13); setting $x_s = 0$ gives

$$g(f_p) = \frac{p(1 - p/c_s)}{2}\sigma^2. \tag{18}$$

The point $g(f_p)$ is the minimum extended-state free energy per length (essentially force) needed to start extending the plectonemic DNA. The f_p that solves this equation is the tension inside a plectonemically supercoiled DNA, and for physiological levels of supercoiling ($\sigma = -0.05$) this force is ≈ 0.5 pN.

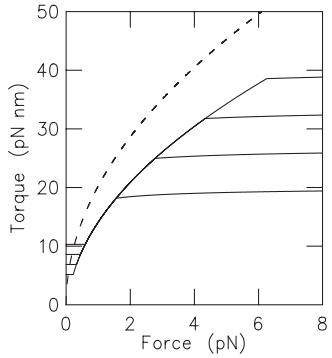

FIG. 3. Torque vs force curve for coexisting state densities corresponding to fixed $\sigma = +0.03$, 0.04, 0.05, and 0.06, with other parameters as in Fig. 2. For forces below the lower critical forces f_p where the extended DNA state disappears (horizontal line segments at left of graph), torque is constant. Above the upper critical force f_s where the plectonemic DNA disappears, the torque slowly approaches its maximum value $(c/\omega_0)\sigma$ (nearly flat regions to right). Between f_p and f_s, the torque follows the same curve for each σ value (concave part of curve). Dashed curve shows $(2k_BTAf)^{1/2}$ for comparison.

As force increases further, the torque will increase as linking number is shifted increasingly from plectoneme to extended DNA, and the torque will be described by Eq. (17). In the coexistence range the torque will be independent of σ.

Finally, when sufficient force f_s is applied, the plectonemic domains will be destroyed; again Eq. (13) can determine this point, by setting $x_s = 1$:

$$g(f_s) = \frac{c_s - p}{2}\sigma^2. \tag{19}$$

The torque at this point will be $\tau_s = (c_s/\omega_0)\sigma$. As the force is increased further, the small amount of linking number remaining will be forced into DNA twist, gradually forcing the molecule torque toward its limit of $\tau = (c/\omega_0)\sigma = k_BTC\omega_0\sigma$.

Figure 3 plots torque versus force for $\sigma = 0.03$, 0.04, 0.05, and 0.06 using the same stiffnesses as used in Fig. 2 ($C = 95$ nm, $A = 50$ nm, $P = 24$ nm). The torque starts at a constant (horizontal segments to left; lowest corresponds to $\sigma = 0.03$; highest to $\sigma = 0.06$). Then, the torque starts to increase when extended DNA starts to be created at f_p. In the coexistence regime, the torque does not depend on σ, so all the curves overlap. When f_s is reached, the torque curves separate again, and then torque only slowly increases with further force increase (nearly horizontal curves to right).

E. The coexisting-state torque is not $(2k_BTAf)^{1/2}$

The torque in the coexistence range of σ, Eq. (17), is not equal to $\tau = (2k_BTAf)^{1/2}$ where A is the bending persistence length as has been suggested in Refs. [8,9,14]. This formula is reminiscent of that for the critical torque for the linear instability of buckling of a rod under tension f from classical elasticity theory, $(4k_BTAf)^{1/2}$ [20,31,32,38], but with the factor of 4 replaced by a 2. The derivation of the formula with the 2 uses an approximate calculation [9] which uses me-

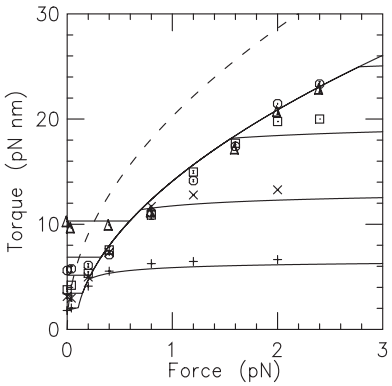

FIG. 4. Comparison of the theoretical torque formula of this paper [solid curve shows Eq. (17); horizontal line segments to left show pure-plectonemic-state torques; to right pure-extended-state torques] with results of MC calculations (symbols) following the method of Ref. [24] for an effective DNA thickness appropriate to describe 200 mM univalent salt solution. MC data are shown for σ=0.01 (+), 0.02 (×), 0.03 (□), 0.04 (○) and 0.06 (△); successively higher pure-state torques are computed for the same linking numbers. Both analytical and MC calculations use A=50 nm and C=95 nm; the analytical calculation uses P=24 nm determined from the MC calculation (see text). Dashed curve shows $(2k_BTAf)^{1/2}$ for comparison.

chanical energy without including effects of thermal fluctuations.

Figure 3 compares the analytical result of this paper, Eq. (17), using P=24 suitable for ≈200 mM univalent salt, with the formula $\tau=(2k_BTAf)^{1/2}$. The latter formula overestimates the torque by roughly 25%. Given the accuracy of single-DNA micromechanical measurements plus the consequences of this overestimate for other measurements, e.g., energy landscape parameters for topoisomerases [14], this discrepancy is significant. A second issue is that the DNA torque, being dependent on the free energies of the coexisting phases, can be expected to depend on factors which shift around those free energies, notably solution ionic conditions. For example, lower-salt solution conditions that produce a larger value of P without changing A or C significantly will bring the coexistence torque closer in value to $(2k_BTAf)^{1/2}$. Direct torque measurements are needed to test Eq. (17) using c_s and g extracted directly from experimental data.

III. COMPARISON OF TORQUE FORMULAS WITH RESULTS OF MONTE CARLO CALCULATION

An alternative to the analytical approach of the preceding sections is to use Monte Carlo (MC) calculation of extension versus linking number and force for DNA [24]. The virtue of a MC approach is that no approximations or empirical assumptions need to be made; the vices include tedium and a lack of physical insight. However, comparison of Eq. (17) with MC results is valuable as a check on the assumptions that go into the analytical theory.

Here, the torque versus force for DNA was calculated using the MC method of Ref. [24], for a 10 kb length DNA and A=50 nm and C=95 nm. The ion concentration indirectly enters the MC calculation through the effective thickness (cross-section diameter) of the double helix. A 5 nm diameter was used, which corresponds to 200 mM univalent salt, approximately physiological salt conditions and comparable to conditions commonly used in biochemistry and single-molecule experiments on supercoiled DNA.

Figure 4 compares the analytical result Eq. (17) with the MC results. MC torque versus force data are shown for σ =0.01 (+), 0.02 (×), 0.03 (□), 0.04 (○), and 0.06 (△). The MC calculation shows the same general behavior as the analytical model, with a low-force constant-torque regime corresponding to pure plectonemic DNA; a high-force nearly-constant-torque regime corresponding to pure extended state; and an intermediate mixed-state regime which is nearly σ independent (collapse of different symbols together).

The results of the theory of the previous section (using the stiffnesses discussed above, C=95 nm, A=50 nm, and P =24 nm) are also shown (solid curves). The central square-root-like curve indicates the coexisting-state torque [Eq. (17)] which is σ independent; MC data in the coexistence regime collapse onto this curve. The horizontal lines that break off to the left of the coexistence curve indicate the constant torques in the pure plectonemic state formed at low force for the same series of σ values as used for the MC calculations, and are in accord with the low-force MC data. The curves that break off to the right of the coexistence torque curve indicate the torques in the pure extended state for the series of σ values used in the MC calculations, and also are in good accord with the MC data.

At zero force, over the range σ=0–0.06 the dependence of τ on σ in the MC calculation rises nearly linearly, with a slope corresponding to $P\approx$24 nm (this can be seen from the nearly linear increments of torque with σ at zero force at the left edge of Fig. 4). Thus when the choice of P=24 nm following from the torque in the pure plectonemic state is plugged into Eq. (17), one describes the MC results for the mixed-state regime quantitatively. By comparison the formula $(2k_BTAf)^{1/2}$ (dashed line) overestimates the torque calculated via MC calculations by more than 25%.

IV. TORQUE-MELTED DNA

For positive supercoiling up to $\sigma\approx$0.1, with tensions in the few piconewton range, the mechanical properties of DNA are remarkably well described by the harmonic bending and twisting model, using single values for $A\approx$50 nm and $C\approx$95 nm. The situation is different for negative supercoiling, where the combination of $\sigma<-0.01$ and forces greater than 1 pN lead to nearly no change of extension with linking number. Strick and co-workers have carried out elegant analyses of the difference between positive and negative supercoiling to extract the free energy of denaturation [7,9].

With only slight modification, the model of the preceding section can be used to analyze negative-supercoil-induced denaturation. The extended state remains, but the plectoneme state is replaced with a denatured-DNA state:

$$\mathcal{D}=\frac{c_d}{2}(\sigma-\sigma_0)^2+\epsilon_d-g_d. \tag{20}$$

Here ϵ_d is the denaturation free energy, which is taken to be $2.0k_BT$ per base pair or per length of B-DNA, ϵ_d

$=6.0k_BT/\text{nm}$ (recall that GC-rich sequences have $\epsilon_d \approx 3.5k_BT/\text{bp}$, while AT-rich sequences have $\epsilon_d \approx 1k_BT/\text{bp}$ [39], so $\epsilon_d=2k_BT$ provides a simple sequence-averaged estimate).

The quantity g_d is analogous to g, except that it describes the polymer properties of denatured (stress-melted) duplex DNA. The polymer elasticity of denatured DNA is certainly modified relative to that of the double helix. Denatured DNA is likely to have a much shorter persistence length, due to its disordered secondary structure. Also, existing experimental data [33,34] indicate that denatured DNA has a contour length per base pair larger than that of B-DNA, due to the straightening of the sugar-phosphate backbones.

Here, denatured DNA is taken to be a semiflexible polymer [5] with a persistence length $A_d=4$ nm, and a contour length per base pair 1.2 times that of B-DNA. The corresponding free energy is

$$g_d = \lambda\left(f - \sqrt{k_BTf/A_d} + \cdots\right), \tag{21}$$

where the leading terms dominate for $f > k_BT/A_d \approx 1$ pN. Here, the exact semiflexible polymer free energy is used (see Ref. [5] for a detailed discussion). The factor $\lambda=1.2$ describes the increased length per base pair due to denaturation.

Once DNA is denatured, its relaxed linking number will not be small; $\sigma_0 \approx -1$ is appropriate for relaxed strand-separated DNA. Finally, c_d describes the twist rigidity of the denatured double helix in a similar way to c_s and p. In general c_d can be considered to be force dependent, although here it is treated as force independent. Since the two single-strand (ss) DNA backbones once denatured are completely flexible, a value of c_d corresponding to a twist persistence length of only a few bases is reasonable. The twist persistence length is here taken to be $c_d/(\omega_0^2 k_BT)=1.75$ nm.

Thus a mixed state of extended and denatured states similar to Eq. (11) occurs:

$$\mathcal{F} = x_s\left(\frac{c_s\sigma_s^2}{2} - g\right) + x_d\left(\frac{c_d}{2}(\sigma_d - \sigma_0)^2 + \epsilon_d - g_d\right). \tag{22}$$

Analogous to the extended-plectonemic coexistence solved above, the equilibrium conditions $\partial\mathcal{F}/\partial x_s=0$ and $\partial\mathcal{F}/\partial\sigma_s=0$ need to be solved, subject to the constraints $x_s+x_d=1$ and $\sigma=x_s\sigma_s+x_d\sigma_d$. This leads to coexisting-state linking number densities

$$\sigma_{s,\mp} = \frac{c_d}{c_s - c_d}\left(-\sigma_0 \mp \sqrt{\sigma_0^2 + \frac{2(c_s - c_d)}{c_s c_d}(g + \epsilon_d - g_d)}\right),$$

$$\sigma_{d,\mp} = \sigma_0 + \frac{c_s}{c_s - c_d}\left(-\sigma_0 \mp \sqrt{\sigma_0^2 + \frac{2(c_s - c_d)}{c_s c_d}(g + \epsilon_d - g_d)}\right). \tag{23}$$

The two branches of solution refer to the two coexistence regions that occur for negative (top sign) and positive (bottom sign) σ; due to the denatured state having $\sigma_0=-1$ there is a strong breaking of σ-reversal symmetry by DNA denaturation. The torques at the denaturation points follow from either the extended or denatured coexistence linking numbers:

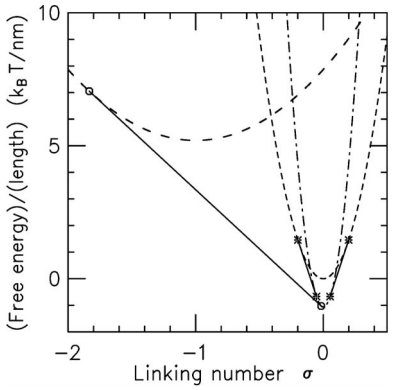

FIG. 5. Free energies of extended (dot-dashed curve), plectonemic (short-dashed curve, minimum at $\sigma=0$), and denatured (long-dashed curve, minimum at $\sigma=-1$) DNA states, for force of 5 pN. Solid straight line segments terminating in stars indicate coexistence regions between extended and plectonemic states. Solid straight line segments terminating in circles indicate coexistence region between extended and underwound denatured states. For negative σ the lowest-energy states are combinations of extended and denatured DNA; the extended-denatured DNA coexistence line is below that for extended-plectonemic states for $\sigma<0$. Because the lowest-energy twist state of denatured DNA has $\sigma_0=-1$, this $\sigma<0$ coexistence occurs between extended DNA of $\sigma \approx -0.02$ and denatured DNA of $\sigma \approx -2$. For $\sigma>0$ the first coexistence that occurs is between extended and plectonemic DNA; for sufficiently large σ a second plectonemic-denatured coexistence occurs but is not shown on this graph.

$$\tau_{d,\mp} = \frac{c_s}{\omega_0}\sigma_{s,\mp} = \frac{c_d}{\omega_0}(\sigma_{d,\mp} - \sigma_0). \tag{24}$$

For $\sigma<0$ the two terms inside the large parentheses of Eq. (23) have opposite signs, so denaturation occurs at a relatively small σ_s. For increasing forces the springlike g_d catches up with the roughly linearly varying g, pulling σ_s to lower values. Note that, when denaturation occurs, σ_d will be appreciably beyond σ_0, since the twist stiffness of the denatured state is much lower than that of extended double helix ($c_d \ll c_s$). This effect can be seen graphically in Fig. 5; the relatively low curvature and minimum position ($\sigma_0=-1$) of the denatured state forces coexistence with extended DNA to occur at $\sigma_d \approx -2$. In the case shown (Fig. 5, force $f=5$ pN, $\epsilon_d=6k_BT/\text{nm}=2k_BT/\text{bp}$, $c_d/k_BT\omega_0^2=1.75$ nm, all other parameters as in the previous section), the appearance of denatured DNA preempts plectonemic supercoiling as the molecule is underwound ($\sigma<0$).

A. Extension versus linking number including denaturation effects

Figure 6(a) shows the extension as a function of linking number, for four forces (0.5, 1.0, 2.0, and 5.0 pN), for stiffnesses $A=50$ nm, $C=95$ nm, and $P=24$ nm. For the lowest force, a transition from extended DNA to plectonemic supercoiling occurs for both signs of σ; denatured DNA is never the lowest free energy state over the range of σ shown, and the extension is symmetric under sign reversal of σ. How-

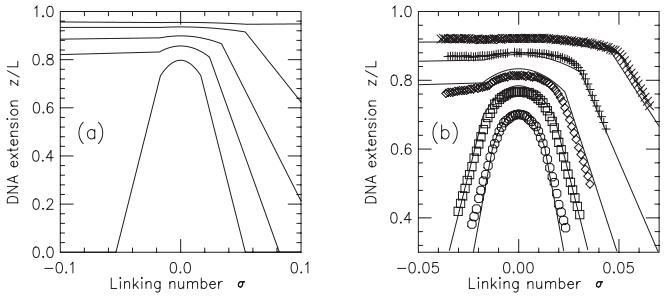

FIG. 6. Extension versus linking number σ for DNA at constant forces. (a) Results of theory for forces of 0.5 (lowest curve), 1, 2, 5, and 10 pN (highest curve), using $A=50$ nm, $C=95$ nm, $P=24$ nm, and denaturation parameters as described in the text. For 0.5 pN the extension is symmetric under sign change of σ, due to coexistence occurring between extended and plectonemically supercoiled DNA states, which have this symmetry. However, for forces of 1, 2, and 5 pN, coexistence occurs between extended and plectonemic DNA for $\sigma>0$, but between extended and denatured DNA for $\sigma<0$, exhibiting a strong breaking of $\sigma\rightarrow-\sigma$ symmetry. Finally for 10 pN, denaturation occurs for both positive and negative σ. (b) Comparison of theoretical results (solid curves) to experimental data of Charvin for 48 kb λ-DNA in 10 mM phosphate buffer (symbols) taken from Ref. [23]. Forces used for experiment and corresponding theoretical curves are 0.25 (○), 0.44 (□), 0.74 (◇), 1.31 (+), and 2.95 pN (×). Parameters as in (a), except for $P=28$ nm which is appropriate for the 10 mM Na^+ buffer.

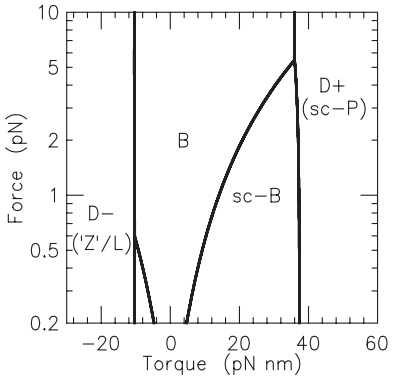

FIG. 7. Force-torque phase diagram showing transitions between extended double helix (B), plectonemically supercoiled B-DNA (scB), underwound denatured DNA (D−), and overwound denatured DNA (D+). Note that the denaturation transitions occur at torques of $\tau_{d,-}\approx-10$ pN nm and $\tau_{d,+}\approx+40$ pN nm. The small triangular region below 0.6 pN and between torques of −5 and −10 pN nm is plectonemically supercoiled B-DNA with negative linking number. The denatured states correspond to the "Z"/L and scP states observed experimentally.

ever, for the larger-force cases, for $\sigma<0$ denaturation of DNA preempts formation of plectonemic supercoils (as shown in Fig. 5). For the opposite sense of winding, $\sigma>0$, the extended-plectonemic state is the lowest free energy state; the result is a strongly asymmetric extension versus linking number response for the higher-force cases, as is observed experimentally [9]. The strong asymmetry between the extension during creation of plectonemic versus denatured DNA arises from the highly disparate levels of linking number that can be stored in those two states. The large value of $\sigma_0=-1$ allows a large amount of linking number to be stored with little change in extension, as seen experimentally [9].

For $\sigma>0$, the denatured phase is less favorable due to the larger amount of twist energy required to make a strongly positively denatured state, in turn due to $\sigma_0=-1$, the basic source of chiral asymmetry in this model. For large enough force [highest force, 10 pN, in Fig. 6(a)], the positively supercoiled denatured state does become favorable to positive plectonemic supercoiling. In this case a state with $\sigma_{d,+}\approx+2$ appears, corresponding to highly overwound denatured DNA.

Figure 6(b) shows the results of the model of this paper using the DNA twisting and bending stiffnesses as above ($A=50$ nm, $C=95$ nm), but with plectonemic stiffness adjusted to the $P=28$ nm appropriate for 10 mM univalent salt [30], compared to experimental data for DNA in 10 mM phosphate buffer (roughly 10 mM univalent salt). The worm-like chain stretching free energy g is determined by A, the Moroz-Nelson result for the extended DNA free energy is determined by A and C, and the denaturation model is as described above. Experimental data shown are due to measurements by Charvin on a 48 kbase λ-DNA presented in Ref. [23], for forces ranging from 0.25 up to 2.95 pN.

Without any fitting (the choices of stiffnesses and the forms for g and c_s are established in other works describing DNA mechanical properties), the extension vs linking number curves observed experimentally are reproduced by the model. For positive supercoiling where denaturation does not occur, the theory depends only on three constants (A, C, and P), the values of which are determined by separate experiments. For negative supercoiling, the denaturation effects are of course also dependent on the parameters in the DNA denaturation model.

B. Denatured states and force-torque "phase diagram"

The model for denatured DNA presented above contains almost no detail concerning how the separated ssDNAs can pack together when highly twisted; the denatured phase is entirely described by the ssDNA polymer elasticity (g_d), the twisting elasticity c, the state of minimum twist energy σ_0, and the denaturation energy ϵ_d. However, this model does describe many features of the denaturation transitions experimentally known to occur for both signs of linking number. The transition for unwinding occurs from a double helix to a state with $\sigma_{d,-}\approx-2$, i.e., to a left-handed double helix of helix repeat of approximately 10 bp. The transition to this state occurs at a torque of about $-2.2k_BT\approx-9$ pN nm. The two parameters $\sigma_{d,-}$ and $\tau_{d,-}$ match those of the denatured extended state found experimentally for underwound stretched DNA [25,26,34].

The overwound denatured state encountered for $\sigma>0$ forms with $\sigma_{d,+}\approx+2$, corresponding to a helix repeat of roughly 3.5 bp. The denaturation torque at which this state is created is $\tau_{d,+}\approx9k_BT\approx36$ pN nm. These properties are remarkably close to those of the "P-DNA" state (more precisely, for these forces, its supercoiled "scP-DNA" form)

found for highly overwound stretched DNA [25,33,34]. Given the quantitative agreement between the transition linking numbers and torques observed experimentally with those associated with this simple model, it appears that the denatured state properties are determined mainly by the melting free energy and the twisting rigidities of B and denatured DNA, and are not strongly dependent on details of how the two strands pack together after their denaturation.

Figure 7 plots the force-torque phase diagram for forces below 10 pN predicted by the model of this paper ($A=50$ nm, $C=95$ nm, $P=24$ nm). This is the continuation to low sub-piconewton forces of the phase diagram for high forces predicted in Ref. [34]. This low-force phase diagram now contains supercoiled B-DNA (scB); the denatured states (D− and D+) are the low-force versions of the extended and $\sigma \approx -2$ "Z" [25,34] state (renamed L-DNA in Ref. [26]) and plectonemically supercoiled P-DNA states, respectively. In addition to extended-plectoneme and extended-denatured transitions, plectoneme-denatured transitions are also shown [the formulas for the plectoneme-denatured transitions are just those of Eqs. (23) and (24) with extended-state properties replaced with those of the plectonemic supercoil, i.e., $g \to 0$ and $c_s \to p$].

V. TORQUE-DRIVEN DNA SWIVELING MEDIATED BY TYPE-I TOPOISOMERASES

Calibrated torques can be used to analyze enzymes that change DNA linking number by allowing controlled rotation of one strand about the other at a point of "nicking" or cutting of one strand. Experiments on type-Ib topoisomerases [14] have demonstrated that such enzymes present sufficient rotational friction that relaxation rates are in the few rotations per second range, and easily measurable. Koster *et al.* have discussed this friction in terms of thermally assisted crossing of a rotational energy barrier. Here a general model is presented for this type of barrier-limited rotation, which indicates that the nonlinear friction must in general be rotation-sense dependent. The average number of rotations that occur when the relaxation is "gated" by transient cleavage and religation of the DNA is also discussed.

A. Molecular rotational friction and DNA swiveling

Following Koster *et al.* [14], during relaxation of positive linking number in a DNA molecule following cleavage, the rotation rate of one strand about the other is limited by the rate of passage over a free energy barrier. Since the barrier has some width, there will be some angle θ_+ from the base of the barrier to its peak. Therefore the relaxation rate (turns per second) will be $r_+ = r_0 \exp[-\beta(G_B - \tau\theta_+)]$, where r_0 is the rate of thermal fluctuations and where $\beta = 1/k_BT$ (the torque in the molecule driving relaxation is taken to have the same sign as the external torque that initially established the linking number, i.e., $\tau > 0$ for $\sigma > 0$). The rate r_0 can be expected to be on the order of the thermal diffusion rate associated with the size of enzyme and DNA involved in the barrier crossing ($\ell \approx 1$ nm), or $r_0 = k_BT/\eta\ell^3$, for fluid viscosity η. The torque acts to reduce the net height of the barrier through an angular "lever arm" θ_+, analogous to the role of force and transition-state position in the theory of force-aided thermal barrier crossing [40].

Rotations may also occur in the opposite direction, adding positive linking number to the DNA. For those rotations the same barrier G_B must be scaled from the other side. The angle between the point of lowest free energy to the peak will be a different value θ_-, reflecting the chirality of the DNA double helix and the enzyme, and giving a negative linking number relaxation rate of $r_- = r_0 \exp[-\beta(G_B + \tau\theta_-)]$. This rate is stimulated by negative torques, and suppressed by positive torques.

Combining the rates of rotation in opposite sense gives the total angular frequency of rotation (defined to be positive for relaxation of positive linking numbers, which generate positive torques in the DNA):

$$\omega = 2\pi(r_+ - r_-) = 2\pi r_0 e^{-\beta G_B}(e^{\beta\tau\theta_+} - e^{-\beta\tau\theta_-})$$
$$= 2\pi r_0 e^{-\beta G_B}\left((\theta_+ + \theta_-)\beta\tau + \frac{1}{2}(\theta_+^2 - \theta_-^2)(\beta\tau)^2 + \frac{1}{6}(\theta_+^3 + \theta_-^3)(\beta\tau)^3 + \cdots \right), \quad (25)$$

where the final equality rewrites the exact formula in a small-$\beta\tau$ expansion.

Inclusion of reverse steps is essential to ensure that the rotation rate goes to zero at zero torque. In the limit of zero rotation rate, the torque varies linearly with the rotation rate ($\tau = \zeta\omega$ for $\beta\tau \to 0$). The linear rotational friction constant is

$$\zeta = \lim_{\omega \to 0} \frac{\tau}{\omega} = \frac{k_BT}{2\pi r_0(\theta_+ + \theta_-)} e^{\beta G_B}. \quad (26)$$

The exponential factor provides a mechanism for generation of large friction, through the low thermal activation rate corresponding to a large G_B. The forward and reverse barrier positions appear symmetrically in ζ. This friction constant is related by the fluctuation-dissipation theorem to the angular diffusion constant $D_r = k_BT/\zeta$.

The nonlinear-τ terms of (25) cause the rotational rate to stray from that predicted by the linear friction constant, once τ reaches the order of k_BT. For large torques the rotation rate becomes larger than the extrapolation of the linear friction, simply because large torque eliminates the effects of the barrier. The asymmetry in the barrier shape ($\theta_+ \neq \theta_-$, expected in the general case given the chirality of DNA and enzymes) causes the first nonlinear friction term to be of order τ^2 rather than the τ^3 that would occur in the chirally symmetric case. The nonlinear rotational friction will thus be different for the two directions of rotation, for any enzyme which mediates a type-I topoisomeraselike rotation of one DNA strand around the other. Equation (25) indicates that this asymmetry can be expected for torques of a few k_BT.

B. Gated swiveling

The previous section describes how torque and angular velocity are related for the case where the rotation requires crossing a free energy barrier, without other constraint. How-

ever, for type-I topoisomerases and other enzymes which cleave one DNA strand, allow some rotations, and then reseal (religate) the cut strand, some finite number of rotations will occur. Following the general scheme outlined by Koster *et al.* [14], suppose that an initial cleavage occurs, followed by rotation of one strand around the other at a rate determined by the friction of the previous section. During each rotation, when the ends come close together, described by a small angular range δ, there is an opportunity for religation at a rate k'. However, while the religated strand is still in the reaction zone of width δ, recleavage can also occur at a rate k. Given an initially cleaved state, the net probability of religation during one turn is

$$P_1 = \frac{k + k' e^{-(k+k')\delta/\omega}}{k + k'}. \tag{27}$$

Here religation and recleavage reactions are assumed to occur only during a time window δ/ω per turn, i.e., during the time that the strand ends are within an angle δ of one another. The results of the previous sections can be used to write this equation in terms of an applied torque τ, or, less directly, in terms of an applied force f. Care should be taken when working in terms of applied force, since even at zero force there is nonzero torque in plectonemically supercoiled DNA (Sec. II).

Given P_1, and assuming independence of the chemical reactions occurring during each turn, the distribution of the number of turns released per initial cleavage is exponential [14]. The average linking number change per relaxation event is

$$\langle \Delta \mathrm{Lk} \rangle = 1/(1 - P_1). \tag{28}$$

Using Eq. (27), as $\omega \to 0$, the average linking number change approaches the limit $\langle \Delta \mathrm{Lk} \rangle_{\omega=0} = 1 + k/k'$ as discussed by Koster *et al.* [14]. If the religation rate k' is much slower than the recleavage rate k then for $\omega \to 0$, $\langle \Delta \mathrm{Lk} \rangle \to k/k' \gg 1$. For large rotation rates $[\omega \gg (k+k')\delta]$, the average linking number change grows linearly with ω, with limiting behavior $\langle \Delta \mathrm{Lk} \rangle = \omega/(\delta k')$.

The recleavage rate k that appears in Eq. (27) may be different from the rate of cleavage at the beginning of the relaxation run, since the enzyme-DNA complex is likely to be in different conformations before the initial cleavage and during the controlled rotation. The two cleavage rates could be independently measured from single-molecule DNA experimental data and it would be interesting to compare them. However, the initial cleavage rate may also be affected simply by the binding-unbinding kinetics of the enzyme to its DNA substrate, possibly making this comparison problematic.

VI. CONCLUSIONS

This paper has presented a simple, closed-form analysis of coexisting domains of different structures in DNA that is twisted and pulled. Section II provides a simple framework indicating how to extract thermodynamic information from experimental data for pulled and twisted DNA. Although established forms for the free energies of extended and supercoiled DNA are used here to prepare figures, and shown to provide a good description of experiments, one could proceed in a largely theory-independent fashion to extract g, P, and c_s directly from extension-σ data at various forces and ionic conditions. This would provide test of existing theories and alternative measurements of these quantities, e.g., [5,28–32].

One such procedure could start with determination of g using force-extension measurements at $\sigma = 0$, or on nicked DNA molecules. Then, measurement of σ_s and σ_p at a given force would determine p and c_s at that force, via Eq. (23). This treats g, p, and c_s as Landau parameters to be extracted from experimental data; their experimentally determined variation with force could test more microscopic theories, e.g., via Eq. (10). It is worth noting that σ_s and σ_p can be measured rather accurately, since they are values of the topological variable σ, the measurement of which involves only counting, without a requirement of precise force or distance calibrations.

Following this scheme, one could likely detect deviations of the σ dependence of the free energies of the plectonemic and extended states from the $O(\sigma^2)$ approximations used in Eqs. (8) and (9). The free energy of supercoiled DNA is dependent on salt concentration [17,28–30]. This effect is largely due to the variation of the effective hard-core diameter of DNA, which becomes larger as salt concentration is decreased due to the increasing range of Coulomb repulsion. As salt concentration is increased, the DNA supercoils become tighter, allowing increased writhe and decreased twisting free energy. By contrast, there should be little effect of univalent salt concentration on the extended-state free energy (i.e., on g and c_s) since the DNA self-interacts relatively weakly when extended.

These effects could be accounted for in a rough approximation by determination of p, which would amount to extraction of the absolute free energy of plectonemic supercoiling and its dependence on salt concentration directly from single-molecule DNA twisting-stretching data. If experimental data demand, it is certainly possible to go beyond the quadratic approximation of Eq. (8), by including σ^3 and σ^4 terms in $\mathcal{P}$ (or in $\mathcal{S}$). Although the equations for state coexistence of Sec. II C might not be analytically solvable in this case, this would allow precise experimental analysis of the free energy of plectonemic supercoiling.

Extension vs linking number measurements published in the literature suggest that there is a salt-concentration-dependent variation of how the slope of the coexistence regions varies with force. In experiments at relatively low salt concentration (10 mM univalent salt) the coexistence regions at different forces have nearly the same slope [9]. Alternately, at higher and more physiological salt concentration (150 mM univalent salt) with Mg^{2+} ions, a gradual variation of the slope of the coexistence regions is observed (see Ref. [23] for a side-by-side comparison of these cases).

The lower-salt behavior may be due to the substantial nonquadratic variation of the plectoneme free energy $\mathcal{P}$ [28]; this will alter the coexistence region slope which for the simple quadratic form of $\mathcal{P}$ varies roughly as $f^{-1/2}$ [see Eq. (13)]. By contrast, for higher salt concentrations the free en-

ergy varies nearly quadratically in σ [28]. In any case, this paper shows how detailed and precise measurements of the free energy of supercoiling can be carried out using single-DNA stretching techniques.

An effect that can be added to the model of Sec. II is the variation of length of the double helix with twist that follows from the chirality of the double helix [41]. This effect, which amounts to a weak breaking of $\sigma \rightarrow -\sigma$ symmetry, has been recently experimentally observed [42,43]. This effect generates a weak coupling of stretching to overwinding, and could be added as a perturbation to the calculation of Sec. II to describe fine details of experimental data. The lowest-order contribution to the free energy generating this effect is a term $\propto -f\sigma$ in the extended state free energy, shifting the free energy minimum to a force-dependent nonzero value of σ. Higher-order-σ terms will be required to describe the nonmonotonicity of this effect seen experimentally [42,43].

Section IV analyzed the strong breaking of $\sigma \rightarrow -\sigma$ symmetry resulting from denaturation of DNA, introducting a simple model for the denatured state involving the known free energy of denaturation, the assumption that denatured DNA takes its lowest free energy when it is entirely unwound ($\sigma=-1$), and the assumption that denatured DNA strands display short (few nm) bending and twisting persistence lengths. The result is that not only is the highly asymmetric extension-σ behavior reproduced [Fig. 6(a)], but also the torques and linking numbers of two denatured DNA states (for $\sigma<0$ the 'Z'/L state [25,34], and for $\sigma>0$ the P state [33,34]) appear in the theory together. This is somewhat surprising given the wide separation of these denatured states in the force-torque phase diagram (Fig. 7) and the crude nature of the model used here to describe them.

The denatured states could be described in more detail, e.g., including explicit inclusion of their characteristic extensions and plectonemic supercoiling [25,33,34]. However, these structural properties appear to play minor roles in determining the denaturation force, torque, and σ values. DNA sequence is known to play a major role in force- and torque-driven denaturation [9], and including sequence effects in the model might be useful for analysis of the $\sigma<0$ extension-torque behavior.

Precise low-force studies of the transitions in the force-torque plane (i.e., testing the predictions of Fig. 7) are now clearly indicated. Recent experimental techniques allowing torque to be indirectly [26] or now even directly [27] controlled should permit the entire phase diagram to be studied. Interesting aspects to explore include the triple points (the points where three transition lines meet in Fig. 7) and the way this low-force phase diagram connects to the high-force force-torque diagram predicted some years ago [34]. The description of the low-force denatured DNA states is a reminder that "overstretched" or S-DNA is distinct from denatured DNA [34].

The approach used in Secs. II and IV need not be considered as connected to particular microscopic models, and can alternately be cast as a general Landau theory of transitions between DNA states. The same calculations with slight variations could be used to describe the twisting-stretching elasticity of protein-DNA complexes. In accord with theoretical predictions based on microscopic models [37,44,45], experiments with DNA-bending proteins have already observed signatures of double-helix twisting [46,47]. The approach of this paper is likely to be useful in analysis of experiments on DNA-protein complexes that twist and writhe DNA.

Finally, Sec. V presented an analysis of the rotary friction and gated rotation mediated by type-Ib-topoisomerase-like enzymes, for a model of molecular-level barrier crossing during rotation similar to that discussed by Koster *et al.* [14]. The additional features of the model of this paper are that it generates the linear dependence of torque on angular frequency required by the fluctuation-dissipation theorem, and that it predicts a particular form of nonlinear friction. An important result is that in general the nonlinear rotary friction encountered for torques in excess of a few k_BT must be different for the two senses of rotation. This may be challenging to definitively demonstrate in experiments where torque is generated by plectonemic supercoils [14] due to the strong asymmetry of the elasticity of DNA itself (i.e., Fig. 7). Use of methods to directly generate constant calibrated torques [27] could allow precise characterization of this effect.

Note added in proof: New experiments [48] have reported different rotation rates for relaxation of positive and negative supercoils in DNA by topo IB in the presence of the drug topotecan, possibly providing a clear realization of the asymmetry discussed in this paper.

ACKNOWLEDGMENTS

Helpful discussions with A. Mondragón and B. Taneja are gratefully acknowledged. This research was supported by NSF Grant No. DMR-0715099.

[1] S. Smith, L. Finzi, and C. Bustamante, Science **258**, 1122 (1992).
[2] C. Bustamante, J. F. Marko, S. Smith, and E. D. Siggia, Science **265**, 1599 (1994).
[3] A. V. Vologodskii, Macromolecules **27**, 5623 (1994).
[4] T. Odijk, Macromolecules **28**, 7016 (1995).
[5] J. F. Marko and E. D. Siggia, Macromolecules **28**, 8759 (1995).
[6] T. R. Strick, J.-F. Allemand, D. Bensimon, A. Bensimon, and V. Croquette, Science **271**, 1835 (1996).
[7] T. R. Strick, J.-F. Allemand, D. Bensimon, and V. Croquette, Biophys. J. **74**, 2016 (1998).
[8] T. Strick, J. F. Allemand, D. Bensimon, R. Lavery, and V. Croquette, Physica A **263**, 392 (1999).
[9] T. R. Strick, J.-F. Allemand, V. Croquette, and D. Bensimon, Prog. Biophys. Mol. Biol. **74**, 115 (2000).
[10] T. R. Strick, V. Croquette, and D. Bensimon, Nature (London) **404**, 901 (2000).

[11] N. J. Crisona, T. R. Strick, D. Bensimon, V. Croquette, and N. R. Cozzarelli, Genes Dev. **14**, 2881-2892 (2000).
[12] N. H. Dekker, V. V. Rybenkov, M. Duguet, N. J. Crisona, N. R. Cozzarelli, D. Bensimon, and V. Croquette, Proc. Natl. Acad. Sci. U.S.A. **99**, 12126 (2002).
[13] N. H. Dekker, T. Viard, C. B. de la Tour, M. Duguet, D. Bensimon, and V. Croquette, J. Mol. Biol. **329**, 271 (2003).
[14] D. A. Koster, V. Croquette, C. Dekker, S. Shuman, and N. H. Dekker, Nature (London) **434**, 671 (2005).
[15] J. Gore, Z. Bryant, M. D. Stone, M. N. Nollmann, N. R. Cozzarelli, and C. Bustamante, Nature (London) **439**, 100 (2006).
[16] J. F. Marko and E. D. Siggia, Science **265**, 506 (1994).
[17] J. F. Marko and E. D. Siggia, Phys. Rev. E **52**, 2912 (1995).
[18] J. F. Marko, Phys. Rev. E **55**, 1758 (1997).
[19] B. Fain, J. Rudnick, and S. Ostlund, Phys. Rev. E **55**, 7364 (1997).
[20] J. F. Marko, Phys. Rev. E **57**, 2134 (1998).
[21] S. Kutter and E. M. Terentjev, Eur. Phys. J. B **21**, 455 (2001); S. Kutter, Ph.D. thesis, University of Cambridge, U.K., 2002.
[22] N. Clauvelin, S. Neukirch, and B. Audoly, in *Proceedings of the Third International Conference on Multiscale Materials Modeling*, edited by P. Gumbsch (Fraunhofer IRB Verlag, Freiburg, Germany, 2006), pp. 605–608.
[23] S. Neukirch, Phys. Rev. Lett. **93**, 198107 (2004).
[24] J. F. Marko and A. Vologodskii, Biophys. J. **73**, 123–132 (1997).
[25] J. F. Léger, G. Romano, A. Sarkar, J. Robert, L. Bourdieu, D. Chatenay, and J. F. Marko, Phys. Rev. Lett. **83**, 1066 (1999).
[26] Z. Bryant, M. D. Stone, J. Gore, S. B. Smith, N. R. Cozzarelli, and C. Bustamante, Nature (London) **424**, 338 (2003).
[27] C. Deufel, S. Forth, C. R. Simmons, S. Dejgosha, and M. D. Wang, Nat. Methods **4**, 223 (2007).
[28] K. V. Klenin, A. V. Vologodskii, V. V. Anshelevich, A. M. Dykhne, and M. D. Frank-Kamenetskii, J. Mol. Biol. **217**, 413 (1991).
[29] A. V. Vologodskii, S. D. Levene, K. V. Klenin, M. Frank-Kamenetskii, and N. R. Cozzarelli, J. Mol. Biol. **227**, 1224 (1992).
[30] V. V. Rybenkov, A. V. Vologodkskii, and N. R. Cozzarelli, Nucleic Acids Res. **25**, 1412 (1997).
[31] J. D. Moroz and P. Nelson, Proc. Natl. Acad. Sci. U.S.A. **94**, 14418 (1997).
[32] J. D. Moroz and P. Nelson, Macromolecules **31**, 6333 (1998).
[33] J. F. Allemand, D. Bensimon, and V. Croquette, Proc. Natl. Acad. Sci. U.S.A. **95**, 14152 (1998).
[34] A. Sarkar, J. F. Léger, D. Chatenay, and J. F. Marko, Phys. Rev. E **63**, 051903 (2001).
[35] L. D. Landau and E. M. Lifshitz, *Theory of Elasticity* (Pergamon, New York, 1986), Chap. 2.
[36] V. Rossetto, Europhys. Lett. **69**, 142 (2005).
[37] J. F. Marko, in *Proceedings of the Les Houches Summer School of Theoretical Physics, LXXXII, August 2-27, 2004, Multiple Aspects of DNA and RNA from Biophysics to Bioinformatics*, edited by D. Chatenay *et al.*, (Elsevier, San Diego, CA, 2005), pp. 248–250.
[38] A. E. H. Love, *A Treatise on the Mathematical Theory of Elasticity* (Dover, New York, 1944), pp. 417–419.
[39] S. Cocco, J. Yan, J. F. Léger, D. Chatenay, and J. F. Marko, Phys. Rev. E **70**, 011910 (2004).
[40] E. Evans and K. Ritchie, Biophys. J. **72**, 1541-1555 (1997).
[41] J. F. Marko, Europhys. Lett. **38**, 183 (1997).
[42] T. Lionnet, S. Joubaud, R. Lavery, D. Bensimon, and V. Croquette, Phys. Rev. Lett. **96**, 178102 (2006).
[43] J. Gore, Z. Bryant, M. Nollmann, M. U. Le, N. R. Cozzarelli, and C. Bustamante, Nature (London) **442**, 836-839 (2006).
[44] S. Cocco, J. F. Marko, R. Monasson, A. Sarkar, and J. Yan, Eur. Phys. J. E **10**, 249 (2003).
[45] J. Yan and J. F. Marko, Phys. Rev. E **68**, 011905 (2003).
[46] G. Charvin, T. R. Strick, D. Bensimon, and V. Croquette, Biophys. J. **89**, 384 (2005).
[47] B. Schnurr, C. Vorgias, and J. Stavans, Biophys. Rev. Lett. **1**, 29 (2006).
[48] D. A. Koster, K. Palle, E. S. M. Bot, M. A. Bjornsti, N. H. Dekker, Nature **448**, 213 (2007).